2954 *Macromolecules* **1996,** *29,* 2954−2959

In Situ Observation of the Orientational Motion of Chromophores during Corona Poling of Electro-Optic Polyimides

Ryoji Inaba,* Masakazu Sagawa, Masato Isogai, and Atsushi Kakuta

Hitachi Research Laboratory, Hitachi Ltd., 7-1-1 Omika-cho,
Hitachi, Ibaraki 319-12, Japan

Received May 31, 1995; Revised Manuscript Received November 27, 1995[⊗]

ABSTRACT: The corona poling process of electro-optic polymers has been investigated for rodlike aromatic polyimides doped with nonlinear optical chromophores. The dynamics of the chromophores in poling during and after imidization was observed by measuring second harmonic generation (SHG) from the polymer. In the course of poling during imidization, the SHG, observed before imidization, decreases to zero, reappears, and increases as the temperature increases. When poling was after imidization, the SHG intensity increased monotonically with increasing temperature. The disappearance of SHG in the poling during imidization is probably due to the known structural change in the polymer chains during imidization and the subsequent reorientation of the chromophores caused by formation of sheets of polyimides. The characteristics of the samples poled during and after imidization are nearly the same in both the extent of the nonlinear susceptibility and their thermal stability.

I. Introduction

Electro-optic (EO) polymers have been widely researched as important materials for future optical communication systems including directional couplers, Mach−Zehnder interferometers, and so on.[1−8] EO polymers are attractive due to their potential for high-bandwidth operation based on their intrinsic low dielectric constant and large nonlinear susceptibilities, as compared with inorganic materials, such as $LiNbO_3$ or GaAs.[2,4,5] They are, in general, polymers doped or labeled with nonlinear optical chromophores. Their second-order nonlinear susceptibilities rely on the alignment of the chromophores induced by electric field poling. Large nonlinearity and high thermal stability are major criteria in selecting the right materials for application to integrated optical devices. Since decay of the EO coefficient is based on the reorientation of the aligned chromophores, polyimides, which are able to retain the alignment of chromophores for long periods of time due to their high glass transition temperature (T_g, ≈ 300 °C), have been widely investigated as host polymers which can improve the thermal stability.[9−15]

Although impressive thermal stabilities for high-T_g polyimide systems have been demonstrated recently, it has also been pointed out that the EO coefficient is not as large as expected in some polyimide systems. This is possibly due to higher order structures of polyimides. Unlike thermoplastic polymers such as poly(methyl methacrylate), the condensation reaction and alignment of the chromophores proceed simultaneously in the poling process of polyimide films. Furthermore, the long axis of the polymer chain is preferentially oriented parallel to the film surface in the imidization reaction for some polyimides.[16−19] This higher order structure change of polymer chains possibly affects the alignment of the chromophores and the magnitude of the second-order nonlinear susceptibilities. It, therefore, should be taken into account in order to improve the second-order nonlinearity. Furthermore, the nonlinear characteristics of polymers should depend on whether the polymers are poled before or after the imidization. However, detailed work on the poling procedure of polyimides is limited,[11] and orientational motion of the chromophores during the poling is still unknown.

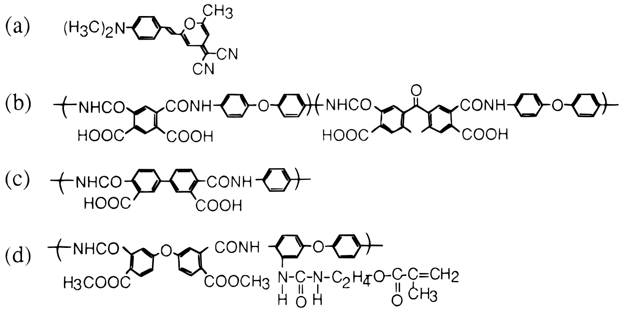

Figure 1. Chemical structures of 4-(dicyanomethylene)-2-methyl-6-(*p*-(dimethylamino)styryl)-4*H*-pyran (DCM) (a) and precursors to aromatic polyimides, PI-1 (b), PI-2 (c), and PI-3 (d), used in this study.

The purpose of this study is to clarify the orientational process of the chromophores in the corona poling of polyimides, which involves the condensation reaction and higher order structural change of polymers on imidization. In a guest−host system, the orientational process of the chromophores is studied by observing second harmonic generation (SHG) from the polymers in the poling during and after the imidization.

II. Experimental Section

1. Sample Preparation. The samples were guest−host polymer systems of 4-(dicyanomethylene)-2-methyl-6-(*p*-(dimethylamino)styryl)-4*H*-pyran (DCM; Figure 1a; purchased from Exciton, Inc.) and precursors to aromatic polyimides (purchased from Hitachi Chemical Co., Ltd.). The chemical structures of the polyimide precursors are shown in Figure 1 (hereafter denoted as PI-1, PI-2, and PI-3). Thin poly(amic acid) films with a DCM content of 10 wt % were prepared as follows.

DCM/PI-1 (Poly(amic acid) Form) Films. The chromophore DCM (30 mg) was dissolved in 2 g of a 1-methyl-2-pyrrolidinone (NMP) solution of PI-1 (poly(amic acid)) with a solids content of 15 wt %. The resulting mixture was stirred for 5 h and spin-cast (for 40 s at 1500 rpm) onto indium tin oxide (ITO) coated glass plates (30 × 30 mm^2). The film was dried in a vacuum oven (<1 Torr) at 70 °C for about 4 h to remove the residual NMP. The average film thickness was ≈6 μm, verified by profilometer thickness measurements.

DCM/PI-2 (Poly(amic acid) Form) Films. DCM/PI-2 film was made from a mixture of 20 mg of DCM and 2 g of a

---

[⊗] Abstract published in *Advance ACS Abstracts,* March 15, 1996.

0024-9297/96/2229-2954$12.00/0

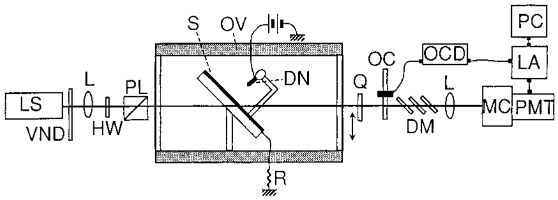

Figure 2. Schematic diagram of the experimental setup for *in situ* observation of the SHG from poled polymers. LS, light source of fundamental 800 nm light; VND, variable neutral density filter; L, lens; PL, polarizer; S, sample; OV, temperature-controlled, N_2-flowing oven; DN, discharging needle; Q, Y-cut quartz crystal; R, resistor; OC, optical chopper; OCD, optical chopper driver; DM, dichroic mirror; MC, monochromator; PMT, photomultiplier tube; LA, lock-in amplifier; PC, personal computer.

NMP solution of PI-2 (poly(amic acid)) (10 wt %) in the same manner as used for DCM/PI-1. The average film thickness was ≈5 μm.

DCM/PI-3 (Poly(amic acid) Form) Films. The DCM (30 mg) and poly(amic acid) of PI-3 (2 g) were dissolved in 2 g of NMP. The film was prepared from the resulting solution in the same way as described above. The average film thickness was ≈2 μm.

DCM/Poly(methyl methacrylate) Films. In order to compare molecular dynamics during the poling of polyimide films with dynamics for a thermoplastic polymer, measurements were also performed for poly(methyl methacrylate) (PMMA) film as a reference sample. The film of DCM/PMMA (10 wt %) was made according to the following procedure. The chromophore DCM (30 mg) and the host polymer PMMA (300 mg) were dissolved in 2 mL of chloroform. The resulting solution was stirred for 4 h and spin cast (for 20 s at 1200 rpm) onto ITO-coated glass plates. The film was dried in a vacuum oven (<1 Torr) at 70 °C for about 3 h to remove the residual solvent. The average film thickness was ≈5 μm. The T_g of this film was ≈80 °C as determined by DSC (differential scanning calorimetric) measurements.

2. Apparatus. The experimental setup is schematically shown in Figure 2. The orientational dynamics of chromophores during the corona poling was monitored *in situ* by observing the SHG signal from a polymer film. The sample-coated glass plate was set in a temperature-controlled, N_2-flowing oven and was held at an angle of 45° relative to the incident laser beam. A discharging needle was set at a distance of 10 mm from the polymer surface. A positive voltage as high as 3.0 kV was applied to the needle during the corona poling.

The light source used as the fundamental radiation was a Ti:sapphire laser, operating at 800 nm with a pulse duration of 100 fs at a repetition rate of 80 MHz. The beam passed through a variable attenuator and a polarizer before reaching the sample. Typical power of the beam was 20 mW, and the beam diameter was ≈1 mm at the sample position. The polarization direction of the incident beam was parallel to the plane of incidence to the film. The transmitted beam was passed through interference filters to remove all traces of the fundamental light before the second harmonic light at 400 nm was detected with a photomultiplier tube. The second harmonic radiation was mechanically chopped by an optical chopper wheel, and the modulated radiation was detected by a lock-in amplifier. A Y-cut quartz crystal was used as a reference sample, and the SHG intensity from poled polymers was normalized using this reference signal.

The temperature of the sample was determined using a thermocouple mounted next to the sample. The ITO electrode was connected to the ground through an 850-kΩ resistor, and the current flow through the polymer was monitored by measuring the voltage drop across the resistor.

III. Results

1. Thermal Gravimetric Analysis of the Chromophore DCM. The thermal gravimetric analysis (TGA) for DCM is shown in Figure 3. The chromophore DCM was heated at a rate of 10 °C/min to obtain the trace of Figure 3a. The results of the isothermal gravimetric analysis are shown in Figure 3b. The weight losses (%) under an isothermal condition in a 0.5 h period were 0.2, 0.5, 1.3, and 4.3 at 200, 220, 240, and 260 °C, respectively. Therefore, the poling or curing process in this study was carried out below 240 °C in order to avoid significant decomposition or sublimation of DCM.

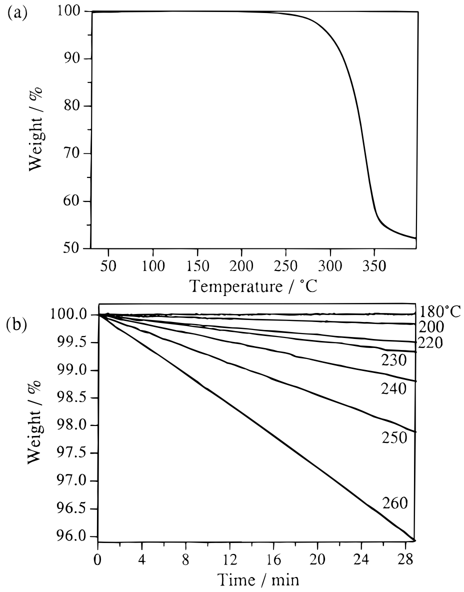

Figure 3. Thermal gravimetric analysis (TGA) for DCM. For the trace in (a), the chromophore DCM was heated at a rate of 10 °C/min. The lines in (b) represent the results of the isothermal gravimetric analysis. The weight losses (%) under isothermal conditions in a 0.5 h period were 0.2, 0.5, 1.3, and 4.3 at 200, 220, 240, and 260 °C, respectively.

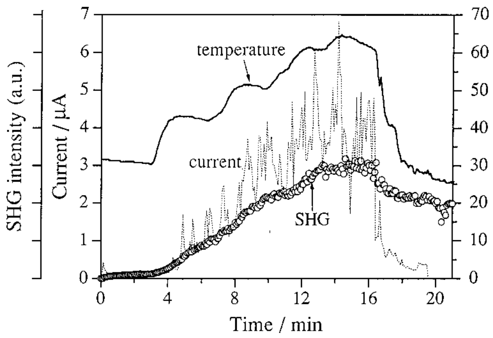

Figure 4. SHG profile in the corona poling of a DCM/PMMA film. The profiles of current and temperature are also shown. The sample was heated in the presence of an electric field. The SHG intensity (open circles, in arbitrary units) and the current through the polymer (dotted curve) are referred to the scale on the left, and the temperature (solid curve) is referred to the scale on the right.

2. Corona Poling of DCM/PMMA Films. The SHG profile in the corona poling of DCM/PMMA was measured in comparison to that of the polyimide film and is shown with profiles of current and temperature in Figure 4. In this poling, the sample was heated from room temperature to 65 °C (15 °C below T_g) in the presence of an electric field. The SHG intensity increased monotonically with increasing temperature. The corona poling was performed below 70 °C, because the surface of the film became opaque above that.

3. Corona Poling of DCM/Poly(amic acid) Films. As described above, the poling of poly(amic acid) films

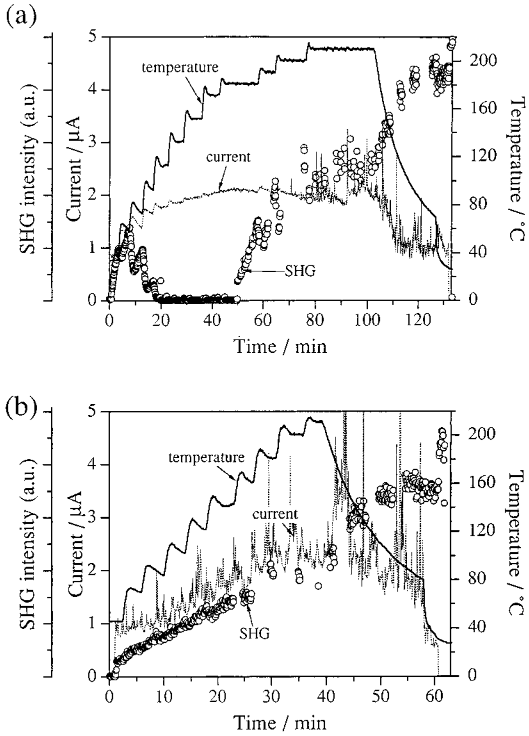

Figure 5. SHG profiles of a DCM/PI-1 film in the poling during (a) and after (b) imidization. The profiles of current and temperature are also shown. The sample was heated in the presence of an electric field.

involves the imidization reaction. Because imidization causes a reduction of free volume available for chromophore occupation,[16-19] the features of orientational dynamics of chromophores in the poling during imidization should differ from those in the poling after imidization. In addition, the samples poled in these two processes might show different thermal stabilities of nonlinearity. Therefore, the SHG intensity profile was observed for the following four stages.

Stage 1: poling during imidization. The poly(amic acid) film was heated gradually from room temperature to ≈220 °C, with +3.0 kV applied to the discharging needle.

Stage 2: orientational decay of chromophores at a heating rate of 10 °C/min. The sample poled in stage 1 was cooled to room temperature, and the dc field was then removed. After the surface charge was removed by rinsing with methanol, the sample was heated at a rate of 10 °C/min.

Stage 3: poling after imidization. The poling field was applied and the sample was heated slowly from room temperature to ≈220 °C.

Stage 4: orientational decay of chromophores at a heating rate of 10 °C/min. The sample poled in stage 3 was cooled to room temperature, and the dc field was then removed. After the surface charge was removed by rinsing with methanol, the sample was heated at a rate of 10 °C/min.

Poling of DCM/PI-1. In Figure 5a, the SHG intensity profile of DCM/PI-1 (poly(amic acid) form) in stage 1 is shown with profiles of current and temperature. As the temperature of the sample increased, the following features were observed in the course of the poling. (i) The SHG was initially observed from room temperature to 80 °C. (ii) A further increase in temperature caused the SHG to disappear above 100 °C. (iii) The SHG was again observed above 180 °C. (iv) The SHG intensity increased as the temperature rose to 210 °C. (v) The SHG intensity increased slightly when the sample was cooled to room temperature. The power of the fundamental which transmitted the sample remained unchanged throughout stage 1. Therefore, there was no scattering loss for the SHG observed in stage 1.

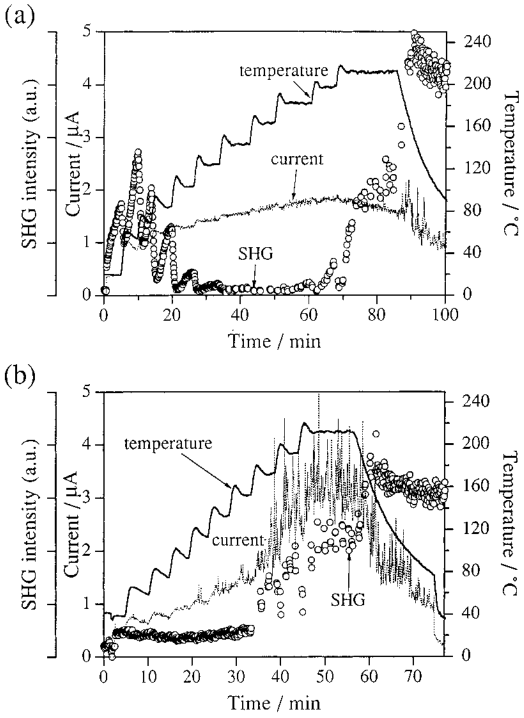

Figure 6. SHG profiles of a DCM/PI-2 film in the poling during (a) and after (b) imidization. The profiles of current and temperature are also shown. The sample was heated in the presence of an electric field.

In Figure 5b, the SHG intensity profile of DCM/PI-1 in stage 3 is shown with profiles of current and temperature. In this case, the SHG intensity increased monotonically with increasing temperature. When the sample was cooled to room temperature, the SHG intensity increased slightly. The SHG intensity immediately after the poling was 70% as much as that measured in stage 1.

Plotted points for the SHG intensity were sparse at temperatures above 190 °C for the following reason. The SHG intensity decreased if the sample was laser irradiated above 190 °C. The sample seemed to decompose. In order to avoid this decomposition, the sample was irradiated only for 10 s when SHG measurements were needed above 190 °C.

Poling of DCM/PI-2. Figures 6a and b show the SHG intensity profiles of DCM/PI-2 in stages 1 and 3, respectively. Profiles of current and temperature during the poling are also shown. These profiles of SHG intensity in stages 1 and 3 were almost identical with those observed for DCM/PI-1. The SHG intensity immediately after the poling was 65% of that measured in stage 1.

Poling of DCM/PI-3. In Figure 7a, the SHG intensity profile of DCM/PI-3 (poly(amic methyl ester) form) in stage 1 is shown with the profiles of current and temperature. The profile of SHG intensity in stage 1 was almost the same as that measured for DCM/PI-1 or DCM/PI-2, except for the following two points. (i) The temperature at which the SHG intensity decreased to zero in stage 1 was about 200 °C, *i.e.*, 100 °C higher than that for the PI-1 or PI-2 film. (ii) The magnitude of SHG intensity after the poling of stage 1 was less

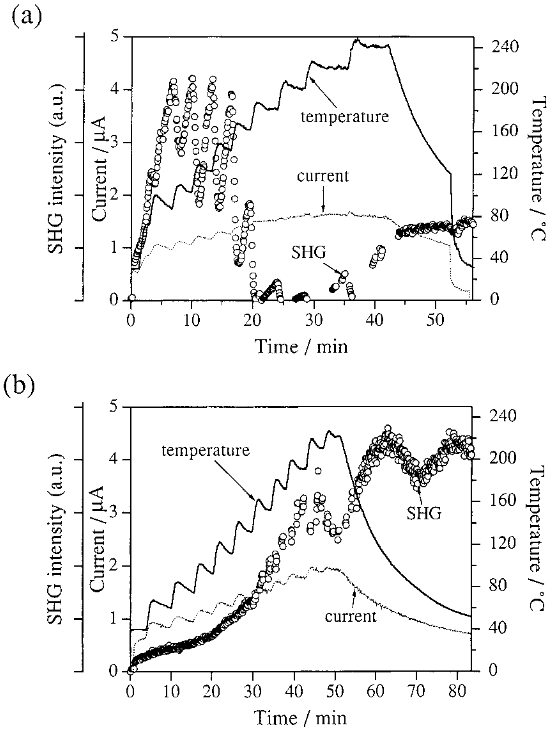

Figure 7. SHG profiles of a DCM/PI-3 film in the poling during (a) and after (b) imidization. The profiles of current and temperature are also shown. The sample was heated in the presence of an electric field.

Table 1. SHG Intensity Observed for EO Polymers and Film Thickness before and after Stage 1

sample	SHG intensity (au)[a] stage 1	stage 3	thickness (μm) before stage 1	after stage 1
DCM/PI-1	0.76	0.52	6.45	4.87
DCM/PI-2	0.42	0.27	5.31	3.57
DCM/PI-3	2.3	1.9	1.92	1.59
DCM/PMMA	50		4.77	

[a] Normalized to the SHG intensity observed from Y-cut quartz inserted in the laser beam line.

than the SHG intensity observed during the poling of stage 1 at around 100 °C.

In Figure 7b, the SHG intensity profile of DCM/PI-3 in stage 3 is shown with the current and temperature profiles. The SHG intensity increased monotonically with increasing temperature, as was observed in stage 3 of PI-1 or PI-2. The SHG intensity soon after the poling was 80% of that measured in stage 1.

4. Relative Intensity of SHG and Its Thermal Stability. Table 1 summarizes the relative intensities of SHG measured after stages 1 and 3. The film thicknesses before and after stage 1 are also listed. The SHG intensity from the sample was normalized to the SHG intensity from the Y-cut quartz inserted in the beam line.

Figures 8 and 9 show the decay profiles of the SHG intensity for DCM/PI-1 and DCM/PI-2, respectively, in stages 2 and 4. The ordinate shows the square root of the SHG intensity, to which the second-order nonlinear susceptibilities are proportional.

IV. Discussion

1. Profiles of the SHG Intensity during Corona Poling. It should be noted that the SHG intensity profile in stage 1 differs significantly from that observed in stage 3 for all the samples; *i.e.*, the poling during imidization and the poling after imidization are quite different processes. The SHG intensity in stage 3 increases monotonically as the temperature increases, very close to the situation observed for the DCM/PMMA film (Figure 4). In stage 1, on the other hand, the SHG, initially observed at the temperature below 100 °C, decreases to zero with increasing temperature. When the sample is heated further to 200 °C, the SHG is observed again.

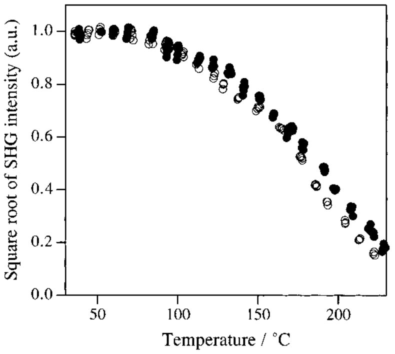

Figure 8. Decay of the SHG intensity in stages 2 (○) and 4 (●) for a DCM/PI-1 film. The sample was heated at a rate of 10 °C/min.

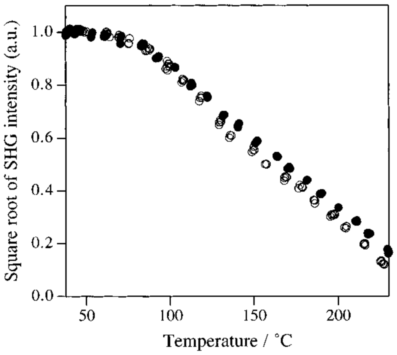

Figure 9. Decay of the SHG intensity in stages 2 (○) and 4 (●) for a DCM/PI-2 film. The sample was heated at a rate of 10 °C/min.

These differences in SHG profiles in stages 1 and 3 might be attributed to the imidization process or higher order structure change of polymer chains. Since the thermal imidization reaction occurs at temperatures above 100 °C for PI-1 or PI-2,[17,20] the imidization of the polymer and alignment of the chromophores proceed simultaneously in stage 1. The polymer chain in poly(amic acid) film is relatively flexible, but as the imidization proceeds, the polymer chain becomes rigid and oriented parallel to the film surface, and sheet structures of polymers are formed.[16-19] As a result, the free volume becomes very small in a direction perpendicular to the film surface. If it is assumed that this structure change of the polymer chains causes the reorientation of the chromophores, the SHG profiles observed in stage 1 can be explained as follows. The rearrangement of polymer chains involved in the imidization reaction overwhelms the alignment of the chromophores poled perpendicular to the film surface before the imidization occurs, causing the decrease in SHG intensity in stage 1 at 100 °C. Because the poly(amic acid) of PI-1 or PI-2 is imidized to about 80% at 210 °C,[17,20] the structure change seems relatively moderate at the temperature around 200 °C. Therefore, as the temperature increases and the polymer becomes mobile, the alignment of the chromophores proceeds and the SHG intensity increases in this temperature region.

The SHG profile in stage 3 is explained as follows. The polymer, at the beginning of stage 3, is almost completely imidized and oriented parallel to the film surface as described above. Therefore, the alignment of the chromophore is not involved in the rearrangement of configuration of the polymer chains as in stage 1. As a result, the chromophores are poled in a small free volume in oriented polymer chains, and the SHG intensity increases monotonically with increasing temperature, *i.e.*, increasing mobility of the polymers. The slight increase in the SHG intensity in the cooling process from 200 °C to room temperature may be the result of diminishing conductivity and increasing internal electric field, as estimated from the decreasing current through the polymers shown in Figures 5−7.

In the poling of PI-3, the temperature at which the SHG intensity decreased to zero in stage 1 is much higher than that of PI-1 or PI-2. This observation is consistent with the results of Becker and Schmidt,[21] who showed that the imidization reaction, in general, occurred at a higher temperature in poly(amic alkyl ester) than in poly(amic acids). It is probable that the difference in the temperature at which imidization occurs differentiates the SHG profile in stage 1 of PI-3 from that of PI-1 or PI-2.

As the imidization reaction proceeds in stage 1, the pH in the polymer films may change, which could affect the magnitude of the hyperpolarizability of the chromophores. This might be related to the increase and decrease profile of the SHG intensity in stage 1. Oscillations in SHG intensity profiles were observed, especially in Figure 7, when the temperature increased in stage 1. The origin of this oscillation is unclear at present. This pH effect might also be involved in this oscillation. This subject is left for furture studies.

Generally, in corona poling, the conductivity of the polymer increases and the internal electric field decreases as the temperature increases, resulting in diminishing poled order of the chromophores. The internal electric field in stage 1 of each sample is thought to be minimized above 180 °C, because the current through the polymer is more than 2 μA above this temperature. (This is the maximum current during the poling.) Since the SHG was observed in this temperature range, the internal electric field was probably sufficient to generate the second harmonic throughout stage 1. Therefore, it is difficult to attribute the significant decrease in the SHG intensity observed at around 100 °C in stage 1 to a reduction of the internal electric field.

The current profile observed in this study was different from that obtained by Stähelin *et al.*,[11] who studied a poling process during imidization. They attributed the decrease in SHG intensity observed in the poling during imidization to a decrease in internal electric field of the sample which caused the reduction of SHG intensity arising from third-order nonlinear effects. In this study, however, the current through the polymer did not change significantly when the SHG decreased at 100 °C, which suggests that the internal electric field remained almost unchanged.

It is unlikely that the origin of the decrease in SHG intensity observed at around 100 °C in stage 1 is the reduction of the film thickness during the imidization as indicated in Table 1. The film thickness was found to be less than the coherent length, because the Maker fringe pattern of the sample after stage 1 did not exhibit an oscillating structure, but just an envelope. The SHG intensity for film thicknesses below the coherent length is proportional to the square of the film thickness while a film shrinkage increases the chromophore density which results in a larger nonlinearity. These combined effects might not result in a drastic change of SHG intensity.

As described above, the effects of the imidization reaction of poly(amic acids) on the electric field poling have been discussed based on the analysis of SHG profiles during poling. From another viewpoint, these observations indicate that SHG measurements show great promise as a means to observe the imidization process or higher order structure changes of polymers. There are many points which remain unclear as to the structure change of polymer chains during the imidization process,[19] and the SHG measurements can be a powerful tool for their clarification. In order to confirm the results obtained in this study, it is necessary to perform *in situ* observations of the dynamics of polymers by polarized infrared spectroscopy.

2. Relative Intensity of SHG. It was found that the samples poled in stages 1 and 3 exhibited nearly the same characteristics in both SHG intensity and thermal stability. This is in contrast to the results obtained by Wu *et al.*,[9] in which they suggested that it was more preferable to pole the films during imidization than to pole the films after imidization in order to achieve good alignment. This was based on the idea that the chromophores poled before imidization might be rigidly fixed by polymers on imidization while the chromophores in the poling after imidization should not be fully poled in the small free volume in imidized polymers. The samples poled in stages 1 and 3 in this study, however, showed nearly the same magnitude of the nonlinearity and thermal stability. This result is explained as follows. As discussed in section IV.A, the poly(amic acid) is almost completely imidized and the configuration of polymers is already rearranged when the chromophores begin to orient at about 200 °C in the poling during imidization (stage 1). This implies that the orientational dynamics of the chromophores in the poling during imidization (stage 1) is essentially the same as in the poling after imidization (stage 3). The polyimide does not function in the same way as a cross-linking polymer, which fixes poled chromophores.[22−26]

It should be noted that the SHG intensity from the DCM/PMMA film, which contained the same amount of chromophores and for which thickness was almost the same as that of DCM/PI-1 film, is 50−100 times as much as that from the polyimide film. As discussed above, the free volume in the polyimides available for the chromophore occupation is estimated to be quite small in the perpendicular direction to the film surface, whether the poling is performed during or after imidization. The origin of the small SHG intensity from the polyimide film is due to the inability of the chromophores, which attempted to align perpendicular to the sheet structure of the polyimides by corona poling, to be fully poled. This result is in agreement with that of the previous work,[9] which suggested that it was difficult to pole the chromophore perpendicular to the film in highly anisotropic polyimides. Stähelin *et al.*[11] suggested that the lower nonlinearity in anisotropic polyimides was due to the difficulty of poling while simultaneously imidizing the conductive poly(amic acid). Comparison of the current profiles in Figures 4 and 5, however, indicates that the conductivity of PMMA film was comparable to that of poly(amic acid) films. Recently, many polyimides, of which second-order nonlinearity is quite large, have been reported.[27−30] Such polyimides include C−C or C−N single bonds in their main chain, and their anisotropy is small. Therefore, the chromophore is easy to align in a direction perpendicular to the film even though the flexibility of the main chain deteriorates the thermal stability of the poled chromophores.

V. Conclusion

The corona poling process of electro-optic polymers was investigated for polyimides of PI-1, PI-2, and PI-3 doped with the nonlinear optical chromophore DCM. The dynamics of the chromophores in poling during and after the imidization was observed by measuring the SHG from the polymer films.

In the process of poling during imidization, alignment of the chromophores was considered to be overwhelmed by the structural change of the polymer chains involved in the imidization reaction. After the poly(amic acid) was almost completely imidized and the sheet structure of the polymers was formed, the chromophore began to orient and the film became SHG-active. This implied that the orientational dynamics of the chromophores in the poling during imidization was essentially the same process as in the poling after imidization. The characteristics of the samples poled during and after imidization were, therefore, nearly the same in both magnitude of the nonlinearity and their thermal stability. The sheet structure of the polymer prevented the orientation of the chromophore so that the SHG intensity from the polyimide film was $^1/_{100}$ to $^1/_{50}$ as small as that from the film of PMMA. In order to increase the magnitude of the second-order nonlinear susceptibilities of polyimide films, it is necessary to introduce another kind of polyimide, chromophore, or way of poling the chromophores.

Acknowledgment. We are grateful to S. Hayashida and M. Taya of Hitachi Chemical Co., Ltd. and H. S. Nalwa, T. Miwa, Y. Okabe, Y. Maekawa, and M. Ishida of Hitachi Research Laboratory for their helpful suggestions and advice.

References and Notes

(1) Burland, D. M.; Miller, R. D.; Walsh, C. A. *Chem. Rev.* **1994**, *94*, 31.
(2) Girton, D. G.; Kwiatkowski, S. L.; Lipscomb, G. F.; Lytel, R. S. *Appl. Phys. Lett.* **1991**, *58*, 1730.
(3) Shuto, Y.; Amano, M.; Kaino, T. *Jpn. J. Appl. Phys.* **1991**, *30*, 320.
(4) Tomme, E. V.; Van Daele, P. P.; Baets, R. G.; Lagasse, P. E. *IEEE J. Quantum Electron.* **1991**, *27*, 778.
(5) Teng, C. C. *Appl. Phys. Lett.* **1992**, *60*, 1538.
(6) Swalen, J. D.; Bjorklund, G. C.; Fleming, W.; Hung, R.; Jurich, M.; Lee, V. Y.; Miller, R. D.; Moerner, W. E.; Morichere, D. Y.; Skumanich, A.; Smith, B. A. *SPIE Proc.* **1992**, *1775*, 369.
(7) Hikita, M.; Shuto, Y.; Amano, M.; Yoshimura, R.; Tomaru, S.; Kozawaguchi, H. *Appl. Phys. Lett.* **1993**, *63*, 1161.
(8) Dubois, J.-C.; Le Barny, P.; Robin, P.; Lemoine, V.; Rajbenbach, H. *Liq. Cryst.* **1993**, *14*, 197.
(9) Wu, J. W.; Valley, J. F.; Ermer, S.; Binkley, E. S.; Kenney, J. T.; Lipscomb, G. F.; Lytel, R. *Appl. Phys. Lett.* **1991**, *58*, 225.
(10) Ermer, S.; Valley, J. F.; Lytel, R.; Lipscomb, G. F.; Van Eck, T. E.; Girton, D. G. *Appl. Phys. Lett.* **1992**, *61*, 2272.
(11) Stähelin, M.; Walsh, C. A.; Burland, D. M.; Miller, R. D.; Twieg, R. J.; Volksen, W. *J. Appl. Phys.* **1993**, *73*, 8471.
(12) Becker, M. W.; Sapochak, L. S.; Ghosen, R.; Xu, C.; Dalton, L. R.; Shi, Y.; Steier, W. H.; Jen, A. K.-Y. *Chem. Mater.* **1994**, *6*, 104.
(13) Hubbard, S. F.; Singer, K. D.; Li, F.; Cheng, S. Z. D.; Harris, F. W. *Appl. Phys. Lett.* **1994**, *65*, 265.
(14) Weder, C.; Neuenschwander, P.; Suter, U. W.; Prêtre, P.; Kaatz, P.; Günter, P. *Macromolecules* **1994**, *27*, 2181.
(15) Yang, S.; Peng, Z.; Yu, L. *Macromolecules* **1994**, *27*, 5858.
(16) Takahashi, N.; Yoon, D. Y.; Parrish, W. *Macromolecules* **1984**, *17*, 2583.
(17) Numata, S.; Fujisaki, K.; Kinjo, N. *Polymer* **1987**, *28*, 2282.
(18) Herminghaus, S.; Boese, D.; Yoon, D. Y.; Smith, B. A. *Appl. Phys. Lett.* **1991**, *59*, 1043.
(19) Hasegawa, M.; Shindo, Y.; Sugimura, T.; Ohshima, S.; Horie, K.; Kochi, M.; Yokota, R.; Mita, I. *J. Polym. Sci., B* **1993**, *31*, 1617.
(20) Numata, S.; Fujisaki, K.; Kinjo, N. In *Polyimides: Synthesis, Characterization, and Applications*; Plenum Press: New York, 1984; Vol. 1, pp 259−271.
(21) Becker, K. H.; Schmidt, H.-W. *Macromolecules* **1992**, *25*, 6784.
(22) Hayashi, A.; Goto, Y.; Nakayama, M.; Sato, H.; Watanabe, T.; Miyata, S. *Macromolecules* **1992**, *25*, 5094.
(23) Muller, S.; Le Barny, P.; Chastaing, E.; Robin, P. *Mol. Eng.* **1992**, *2*, 251.
(24) Aramaki, S.; Okamoto, Y.; Murayama, T. *Jpn. J. Appl. Phys.* **1994**, *33*, 5759.
(25) Hsiue, G. H.; Kuo, J. K.; Jeng, R. J.; Chen, J. I.; Jiang, X. L.; Marturunkakul, S.; Kumar, J.; Tripathy, S. K. *Chem. Mater.* **1994**, *6*, 884.
(26) Wang, W.; Chen, D.; Fetterman, H. R.; Shi, Y.; Steier, W. H.; Dalton, L. R. *Appl. Phys. Lett.* **1994**, *65*, 929.
(27) Jen, A. K.-Y.; Liu, Y.-J.; Cai, Y.; Rao, V. P.; Dalton, L. R. *J. Chem. Soc., Chem. Commun.* **1994**, 2711.
(28) Verbiest, T.; Burland, D. M.; Jurich, M. C.; Lee, V. Y.; Miller, R. D.; Volksen, W. *Science* **1995**, *268*, 1604.
(29) Chen, T.-A.; Jen, A. K.-Y.; Cai, Y. *J. Am. Chem. Soc.* **1995**, *117*, 7295.
(30) Yu, D.; Gharavi, A.; Yu, L. *Macromolecules* **1995**, *28*, 784.

MA950748F